STATE RESEARCH CENTER OF RUSSIA

INSTITUTE FOR HIGH ENERGY PHYSICS

IHEP 96-13

S.V.Golovkin[1], E.A.Kushnirenko[1], A.I.Pyshchev[2], V.M.Shershukov[3],
A.S.Solov'ev[4], V.G.Vasil'chenko[1], A.E.Zibert[2], K.V.Zimyn[1]

NEW LIQUID SCINTILLATORS FOR PARTICLE DETECTORS BASED ON CAPILLARY FIBERS

---

[1] Institute for High Energy Physics, 142284 Protvino, Russia
[2] Institute for Physical and Organic Chemistry, 344104, Rostov-na-Donu, Russia
[3] Institute for Monocrystals, 310001 Khar'kov, Ukraine
[4] Joint Institute for Nuclear Research, 141980 Dubna, Russia

Protvino 1996

UDK 539.1.074.13 M–24

Abstract

Golovkin S.V. et al. New Liquid Scintillators for Particle Detectors Based on Capillary Fibers: IHEP Preprint 96-13. – Protvino, 1996. – p. 17, figs. 12, tables 3, refs.: 17.

A study on optical and luminescent properties of liquid scintillators to be used in tracking detectors and calorimeters is presented. About 60 new scintillating dyes and 8 solvents have been investigated. Liquid scintillators based on 1-methylnaphthalene and a new IPN solvent containing 3M-15, R45, R6 and R39 dyes showed the scintillation efficiency of 34-52% higher relative to the standard polystyrene scintillator. Quartz 0.5 mm capillaries filled with IPN + 3 g/l 3M-15 liquid scintillator exhibited the light attenuation length of about 3.2 m. The decay time constants of the liquid scintillators were about 6.2-7.6 ns. Vacuumed liquid scintillators based on 1-methylnaphthalene enhanced their scintillation efficiencies up to 24-32% relative to those in air. A comparison between liquid-core scintillating fibers and plastic fibers is presented.

Аннотация

Головкин С.В. и др. Новые жидкие сцинтилляторы для детекторов частиц на основе капиллярных волокон: Препринт ИФВЭ 96-13. – Протвино, 1996. – 17 с., 12 рис., 3 табл., библиогр.: 17.

Исследованы люминесцентные и оптические характеристики жидких сцинтилляторов, предназначенных для применения в трековых детекторах и калориметрах. Было изучено восемь различных растворителей и около 60 сцинтилляционных добавок. Сцинтилляционная эффективность сцинтилляторов на основе 1-метилнафталина и нового растворителя IPN с добавками R6, R45, R39 и 3M-15 на 34-52% выше стандартного полистирольного сцинтиллятора. Достигнуты значения длины затухания около 3.2 м для 0.5 мм-капилляров, заполненных жидким сцинтиллятором 1PN + 3 г/л 3M-15. Характерные времена высвечивания для жидких сцинтилляторов составляют 6.2-7.6 нс. Сцинтилляционная эффективность вакуумизированных жидких сцинтилляторов на основе 1-метилнафталина на 24-32% выше по сравнению с их уровнем на воздухе. Проведено сравнение капилляров, заполненных жидкими сцинтилляторами, и пластмассовых сцинтилляционных волокон.

Introduction

During the last few years interest in research and development of particle detectors based on capillary fibers filled with liquid scintillators (LSs) [1-12] has been renewed. The main advantages of such liquid-core capillary fibers can be formulated as follows:

- high level of scintillation efficiency;
- large attenuation lengths l_{att} in liquid-core fibers;
- relatively short decay time constants τ;
- high level of radiation hardness $\geq$100 Mrad;
- high spatial resolution for tracking detectors based on capillaries with small diameters.

For large size particle detectors it is necessary to have a high level of the light output from far ends (2-3 m) of liquid-core fibers. The light output from fibers far ends depends on LSs scintillation efficiency, light trapping efficiency, light attenuation length and etc. The scintillation light trapping efficiency ε in liquid-core fibers is determined by the formula

$$\varepsilon = 1/2(1 - n_{cl}^2/n_{core}^2), \tag{1}$$

where n_{cl} and n_{core} are the refractive indexes of capillary glass walls and LS, respectively. As is clear from (1) there are certain requirements on LSs optical characteristics, i.e. their high refractive indexes. Expression (1) shows that n_{core} must be much grater than n_{cl} in order to obtain high levels of the trapping efficiency. Note that the refractive index of capillary quartz walls is n_{cl}=1.46 and capillary glass walls is n_{cl}=1.46-1.51. It is easy to calculate that quartz capillaries filled with an LS based on 1MN solvent with n_{core}=1.617 (for other refractive indexes of our LSs see Table 2) provide a relatively high level of ε=9.3%, while for polystyrene fibers having an ordinary acrylic cladding (n_{core}=1.59 and n_{cl}=1.49), ε is only 6.1%. Abbreviations and formulae of the used solvents and dyes with their known values of the light absorption maximum λ_{abs}, emission maximum λ_{em} and etc. are presented in Appendix.

The main requirements for a scintillating dye can be formulated as follows: a high level of light yield, large Stocks shift between emission and absorption spectra and high optical transparency of an LS (for its emission spectrum). Fig.1 illustrates transmission properties of some solvents like 1MN, 1PN and DIPN of 1 cm thick layer. This figure shows that the emission spectrum of an LS must be in a wavelength region of λ_{min} >400-460 nm.

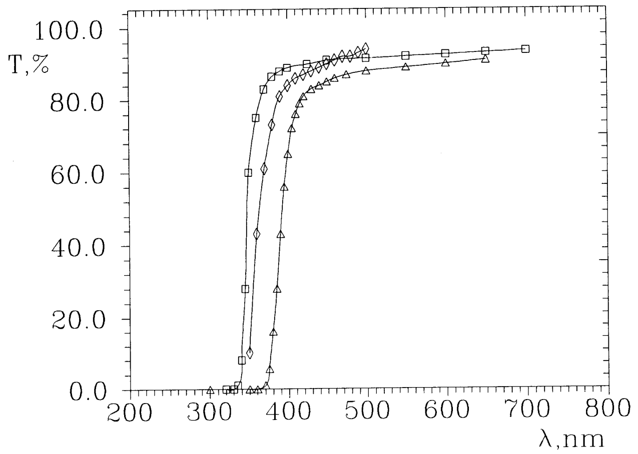

Fig. 1. Transmission properties of some 10 mm thick solvents: □ – 1MN, Δ – 1PN and ◊ – DIPN.

For some detectors which use image intensifiers (IIs) as photoreceivers, one should take into account the transmission properties of II fiber-optic entrance windows. In our case the shortwave cut-off threshold of the II fiber-optic entrance window is λ_{min} ≅400 nm.

All this points out that the maximum emission spectra λ_{max} of our luminescent dyes should lie in a green-orange wavelength region. On the one hand the use of dyes with longer wavelength emission spectra leads to improvements of LSs light attenuation and radiation hardness. On the other hand the quantum efficiency of commonly used IIs and photomultipliers (PMs) in the orange region is noticeably lower. That is the reason for the dyes having their luminescent spectra in the green region to be an optimal choice for the above applications.

The light emission locality, especially for high resolution tracking detectors with 20-50 μm diameter capillaries, is an important factor. It is common knowledge that the use of LSs having a single scintillating dye under high concentration can satisfy the locality light emission requirements when the dominating mechanism of energy transfer from the solvent to the dye is nonradiative. By this is meant that with the increase in the dye concentration the luminescence is localized which prevents the remission of light from one capillary to another. Thus this concentration enhancement leads to a lower level of light attenuation. All these requirements can be satisfied only on the base of a compromise between the concentration of dyes in LSs and their transmission and luminescent properties.

The light output from fibers far ends is another important factor for a tracking detector based on liquid-core fibers. That is why LS light attenuation length l_{att} in fibers is one of the most important characteristics. The value of l_{att} is determined by the inner surface quality of capillaries (the smoothness of inner surfaces and stability of the inner diameters in capillaries), the purity of the used solvent and scintillating dye, the Stocks shift between the absorption and emission spectra of the dye. The influence of these factors on optical and luminescent characteristics of liquid-core scintillating fibers is the subject of this investigation.

Stringent requirements on the radiation hardness of capillaries filled with LSs are imposed for the above applications. The integral dose during the entire time of tracking detectors irradiation for the future generation of colliding beams and fixed target experiments will reach hundreds of Mrad. Some results of the radiation hardness investigation of our LSs and capillaries were presented elsewhere [10]. It was found that the radiation hardness of capillaries filled with our best LSs more than by an order of magnitude exceeded the radiation resistance of commonly used plastic scintillators. For example, the scintillation efficiency of LS based on 1MN + R39 was reduced only by 30% after a dose of 190 Mrad [10].

Taking into account a possibility to use such detectors in high counting rate conditions of about 10^6-10^8 particles/s, a need to find LSs with short decay time constants arises. The temperature stability of LSs light output is of grate importance for some applications (EM-calorimeters, etc.). These characteristics of our LSs were also investigated.

This paper is an account of our search for promising LSs for liquid-core capillary detectors. When summarizing the data on high resolution tracking detectors [7,9,11,12] it became clear that this type of detector was very promising. So some liquid-core capillaries provide $l_{att} \geq 3$ m and the hit density of about 3/mm at a length of 2 m for a bundle of capillaries of $\emptyset$=20 μm in diameter [9]. For a bundle of capillaries of $\emptyset$=16 μm the spatial resolution is about 14 μm/hit [7].

1. Experimental procedure

The scintillation efficiency I_o of our new LSs was measured by exciting LSs samples ($\sim$2 cm^3) with a ^{90}Sr radioactive β-source (in room temperature air). The source and samples were fixed upon the entrance window of a photoreceiver, an image intensifier (II), having the maximum quantum efficiency of its multialkaline photocathode in the green region ($\sim$500 nm). The scintillation output of our new LSs was measured in comparison with a standard polystyrene (PS) scintillator ($\sim$2 cm^3) having 1.5% pTP + 0.01% POPOP. The light output of the PS scintillator was set equal to 100%. The amplified light from the II output window was detected by a PM FEU-85. The PM photocurrent was measured. The instrumentation error of the scintillation efficiency determination was about ±3% with a possible systematic error of about ±5%.

For the light attenuation length measurements of our liquid-core fibers a special setup was used [10]. The fibers were excited by a collimated ^{90}Sr radioactive β-source moving along them. The light attenuation of our LSs was measured in quartz capillaries of $\emptyset$=500 μm and wall thickness of about 60 μm.

The decay time constants of our LSs were measured by the single photoelectron delayed-coincidence technique [13] with FEU-71 PMs having quartz entrance windows. The time resolution of our experimental setup was about 1 ns and the accuracy of decay time constants measurements was about ±5%.

2. Experimental results

2.1. Search for new promising dyes and solvents

At the first stage of our investigation we measured the light output I_o of all available scintillating dyes with 1MN solvent at a concentration of 3 g/l. Experimental results are presented in Table 1.

Table 1. Scintillation properties of LSs based on 1MN.

№	Dyes	I_o, %	№	Dyes	I_o, %
1	BDPAD	148	30	TPB	22
2	BDPD	76	31	L7	142
3	PMP	137	32	L8	110
4	bis-DAPD	105	33	L9	117
5	SFPDMAPO	124	34	L10	37
6	BPEA	125	35	L11	85
7	CLBPEA	120	36	L13	100
8	DMBPEA	111	37	OPBPP	137
9	K-30	147	38	OPBD	130
10	K-7	133	39	R-911	105
11	DSP	149	40	R-912	101
12	DPA	81	41	R-913	107
13	X25	115	42	R-914	94
14	X26	59	43	L15	115
15	X27	82	44	K-27	136
16	R6	145	45	P-26	114
17	R2	162	46	N/266	139
18	oPOPOP	113	47	3M-15	134
19	X31	127	48	OP-45	132
20	3HF	64	49	R63	124
21	R39	152	50	R6-J	119
22	R40	73	51	N/116	57
23	X42	87	52	vPOPOP	81
24	X43	159	53	N/118	15
25	X44	74	54	N/119	49
26	R45	143	55	N/120	110
27	R49	88	56	DMPOPOP	130
28	PPPyr	140			
29	BPPyr	138			

Most of them are dyes emitting light in the green wavelength region. We also investigated dyes emitting light in the blue (bis-DAPD, etc.) region. It was found that they were not efficient. Then a group of the most efficient dyes (with high levels of purity) was submitted to further investigation of their optical properties.

Some efficient dyes like R2, X43, etc. had to be excluded from the group due to their poor light attenuation properties. They showed more than 2 times lower levels of l_{att} in comparison with the remaining ones. These low values of LSs light attenuation were due to low levels of the dyes Stock shifts. On the base of these light output and light attenuation lengths measurements in $\emptyset$=0.5 mm quartz capillaries, the most efficient dyes were chosen, i.e. R6, R39, R45 and 3M-15.

Table 2. Optical and scintillation properties of some LSs.

№	Solvent	Dye	I_o, %	τ, ns	l_{att}, m
1	1MN	R6	145	7.6	1.63
2	n_{core}=1.617	R45	143	6.8	2.87
3		R39	152	6.8	1.88
4		3M-15	134	6.5	2.85
5	IPN	R6	145	6.3	2.01
6	n_{core}=1.59	R45	135	6.2	2.72
7		R39	147	6.2	2.13
8		3M-15	150	6.2	3.19
9	IBP	R6	117		1.20
10	n_{core}=1.59	R2	108		1.10
11		PMP	114		0.73
12	1PN	R6	108		0.67
13	n_{core}=1.63	R45	110		2.01
14		R39	141		0.96
15	1CLN	R6	65		1.56
	$n_{core} = 1.6$				
16	1MON	R6	87		
17	n_{core}=1.62	R45	75		
18		R39	80		
19		3M-15	79		
20	DIPN	R6	118		0.96
21	n_{core}=1.569	R45	111		
22		R39	111		
23		3M-15	102		
24	HnTP	R6	49		0.66
25	n_{core}=1.568	R45	23		
26		R39	19		
27		3M-15	17		
28	50% 1MN + 50% N	R6	98		
29	50% 1MN + 50% DBNB	R6	8		

At the second stage of this investigation we prepared LSs based on all available solvents and the chosen group of dyes with a concentration of about 3g/l. We measured their light output and for the best ones — the main decay time constants and light attenuation lengths l_{att} in $\emptyset$=0.5 mm quartz capillaries. Some measurement results of LSs based on different solvents are presented in Table 2.

As is clear from the data presented in Table 2 the most efficient LSs are based on 1MN and IPN solvents. The light output I_o of LSs based on 1MN and IPN with the promising dyes is practically the same. The highest levels of I_o have LSs like IPN + 3g/l R39 (I_o=147%), 1MN + 3g/l R39 (I_o=152%) and IPN + 3g/l 3M-15 (I_o=150%).

There is a possibility to create new LSs based on complex solvents. So we investigated a possibility of the dissolution of N or DBNB at high concentration ($\sim$ 50%) in 1MN + 3g/l R6. This would allow one to change the refractive index n_{core} of new complex LSs and as a consequence of it would allow one to change their trapping efficiency ε. Some results of new complex LSs characteristics measurements are shown in Table 2. Note that these new complex solvents have low levels of the light output and exist as liquids only at a temperature over 40^{o}C.

We also tested a possibility to load some of our LSs with heavy metal containing dopants like TPT and TPL. Such LSs would allow one to increase low energy γ-quanta detection efficiency. The maximum concentrations of TPT and TPL which could be solved in 1MN + 3g/l R6 were about 2% and 1%, respectively. Note that the use of these dopants has not significantly changed the light output of these LSs in comparison with I_o for 1MN + 3g/l R6 presented in Table 2.

2.2. Light emission locality and choice of optimum dye concentration

It is well known that the light yield of LSs greatly depends on the concentration of solved dyes [1]. Some of the light yield measurements versus the concentration of our promising dyes (with ordinary levels of purity) in LSs are presented in Figs.2a-2b. Our investigations show that the scintillation efficiency of the bulk of promising LSs have practically reached their maximum at dyes concentration $\geq$3 g/l. Only IPN + 3M-15 has its efficiency maximum at a concentration of about 2 g/l. That is why we have chosen this level of dyes concentration, i.e. 3 g/l, in the above measurements.

A knowledge of the function of a LS scintillation efficiency I_o versus the dye concentration allows one to estimate the probability for the excitation energy transfer to the dye by the nonradiative way. For low concentrations, i.e. with a negligible self-quenching of the solute fluorescence when the total light emitted by an LS is captured by the dye, this function is given by formula [14]:

$$I_o \sim (q_{ox} + K * c * \tau_{ox})/(1 + K * c * \tau_{ox}), \qquad (2)$$

where q_{ox} is the solvent quantum light yield, K is the rate constant of the nonradiative energy transfer from the solvent to the dye, τ_{ox} is the decay time constant of the solvent in the absence of a dye and c is the dye concentration. The value of $K * \tau_{ox}$ can be determined from experimental curves $I_o(c)$. The probability η for the nonradiative way of the energy transfer from the solvent to the dye is given by formula [14]:

$$\eta = K * c/(1/\tau + K * c) = K * c * \tau_{ox}/(1 + K * c * \tau_{ox}). \qquad (3)$$

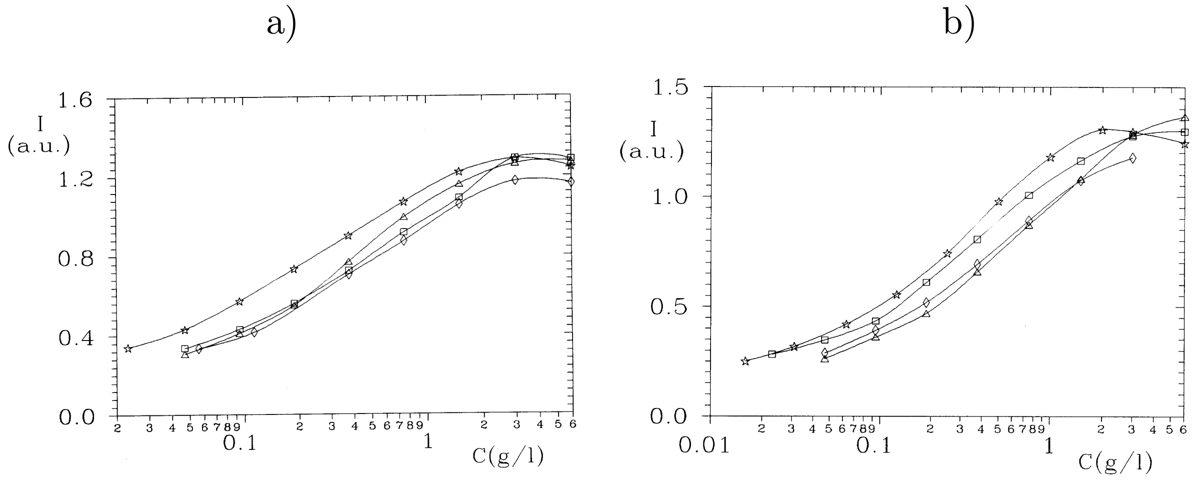

Fig. 2. Light output of some liquid scintillators versus the concentration of dyes: a) □ – 1MN+R6; ☆ – 1MN+R45;Δ – 1MN+R39;◇ – 1MN+3M-15 and b) □ – IPN+R6;◇ – IPN+R45;Δ – IPN+R39;☆ – IPN+3M-15.

This expression allows one to estimate η for each c. With the use of the experimental data presented in Fig.2a-2b, probabilities η for some LSs were estimated. Other data of these probabilities estimation are summarized in Table 3.

Table 3. Probabilities for the nonradiative way of the energy transfer from the solvent to the dye.

№	Scintillators	c, g/l	η
1	IPN + 3M-15	3	0.75
2	IPN + 3M-15	2	0.67
3	IPN + R39	3	0.70
4	1MN + 3M-15	3	0.73
5	1MN + 3M-15	2	0.64
6	1MN + R45	3	0.65
7	1MN + R39	3	0.66
8	1MN + R6	3	0.66

Note that the probability η can be also estimated with the use of data on the decay time measurements which are presented below. Note that the lowest physical limit for the track localization accuracy is determined by the appearance of energetic δ-electrons. For capillaries of $\emptyset$=30 μm the δ-electrons contribution to the fraction of light outside a track is about 10% [15].

2.3. Decay time constant measurements and light emission locality

Fig.3 presents a typical decay curve for 1MN + 3 g/l 3M-15 (in air). These measurements have shown that the main part of our LSs light emission can be fitted with the help of a single decay time constant. Note that decay curves for plastic scintillators have two decay time constants, i.e. about 85-90% of the emitted light has short decay time constants of about τ=3-8 ns and 10-15% of the rest has long ones of about τ_l=30-40 ns. Under high counting rate operation, the presence of intense light emission with long decay time constants may lead to a pile-up of events. For our LSs the contribution of long decay components (with τ_l=30-60 ns) is less than 5%.

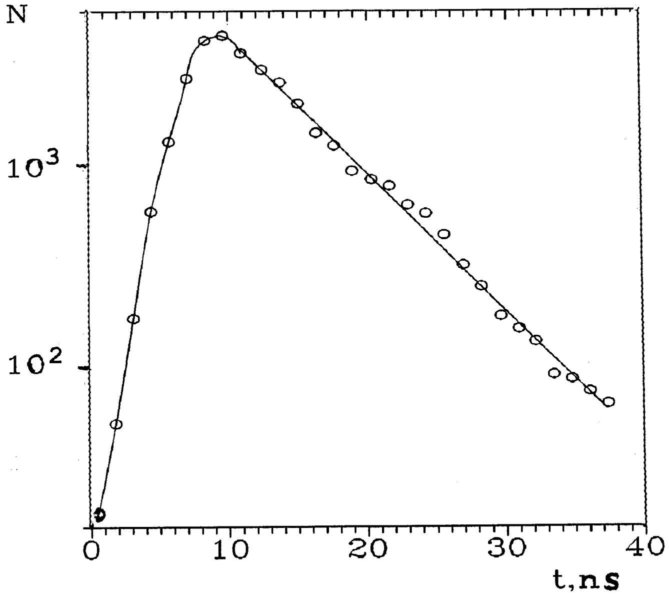

Fig. 3. Decay curve for 1MN+3g/l 3M-15.

All other results are shown in Table 2. As is evident from Table 2, the main decay time constants for our promising LSs based on 1MN and IPN are in a region of τ=6.2÷7.6 ns. The experimental results on decay time measurements for 1MN + 3 g/l R39 and 1MN + 3 g/l R45 were presented elsewhere [8]. It is necessary to emphasize that the decay time constants of LSs depend on dyes concentration. Under the chosen concentration of 3 g/l scintillation pulses durations of our promising LSs are comparable with well known green plastic scintillators like Kuraray-3HF [8].

For the light emission locality estimation based on the decay time measurements, one can note that the main decay time constant of a solvent τ versus the dye concentration is given by expression [4]:

$$1/\tau = 1/\tau_{ox} + K * c. \tag{4}$$

In some cases the decay curve of LSs I(t) can be fitted by expression

$$I(t) \sim \Big(exp(-1/\tau) - exp(-1/\tau_y)\Big)/\Big(\tau - \tau_y\Big), \tag{5}$$

where τ_y is the dye decay time constant. The use of experimental function $I(t)$ for different dye concentrations allows one to find $\tau(c)$ from expression (5) and K from expression (4). Thus, the probability of the energy transfer by the nonradiative way η is determined from equation (3). Note that some experimental data on $I(t)$ curves measurements were also presented elsewhere [8]. With the use of decay time measurements data it is easy to find that probabilities of the energy transfer by the nonradiative way for 1MN + 3 g/l R45 and 1MN + 3 g/l R39 are η=0.61 and η=0.66, respectively. These results are in a good agreement with the data presented in Table 3.

The above data can be also used to estimate the absorption length l_o for light emitted by the solvent. We measured the absorption spectra of LSs thin layers (~25 μm) and estimated the decadic molar extinction coefficient ε (l mol^{-1}cm^{-1}) which is determined by the equation:

$$A = A_o * exp(-\varepsilon * c * s * ln10), \tag{6}$$

where A_o is the initial intensity of light emitted by the solvent, s is the thickness of a layer (cm) and c is the concentration of the dye (mol/l). At the maximum of 1MN emission spectrum one obtains ε=1.03·10^4 l mol^{-1}cm^{-1} for R6. Taking into account the dye concentration of about 3 g/l one can calculate $l_o = 1/(\varepsilon * c * ln10)$, which is about $l_o = 59$ μm.

2.4. Light attenuation length in liquid-core capillaries

2.4.1. Influence of LS purity, dye concentration and capillaries quality on light attenuation

The quality of used solvents and scintillation dyes plays an important role in the light output and light attenuation of liquid-core capillary fibers. We investigated the influence of different purification methods of solvents on LSs light attenuation lengths. Fig.4 shows some of these experimental results of the light attenuation measurements in $\emptyset$=0.5 mm capillaries for several samples of differently purified IPN solvent (with R45 dye at a concentration of 3 g/l). We found a purification method which allowed us to improve IPN + 3 g/l R45 light attenuation length over 10 times and to reach a level of $l_{att} \geq 3$ m, i.e. to increase the light output from 1 m fiber over 33 times.

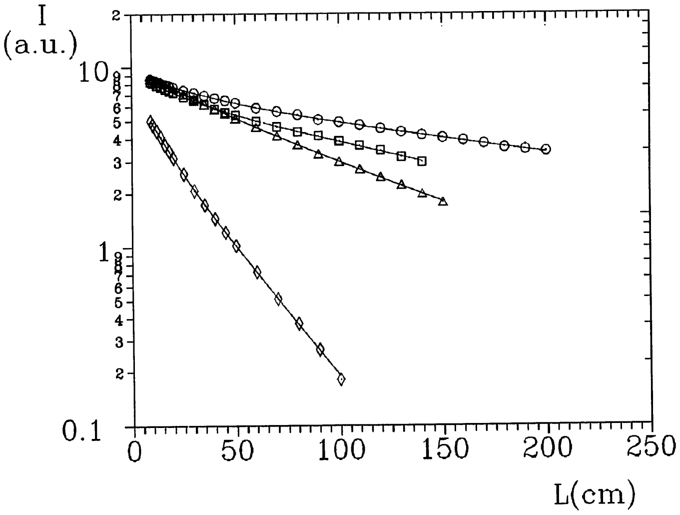

Fig. 4. Influence of solvent purity on lightattenuation lengths: o – IPN (high purity)+3g/l R45 l_{att}=2.72 m; □ – IPN (ordinary purity)+3g/l R45 l_{att}=1.65 m; Δ – IPN (intermediate purity)+3g/l R45 l_{att}=1.04 m and ◊ IPN (low purity)+3g/l R45 l_{att}=0.3 m.

We also tested the influence of R45 dye purity on the light attenuation in liquid-core capillaries. Some of our experimental results are presented in Fig.5. The best dye purification method allowed us to increase the light attenuation length for 1PN +3g/l R45 about 1.2 times.

We investigated the influence of our capillary quality on the light attenuation in liquid-core capillary fibers. Capillaries were specially treated before filling them with 1MN + 3 g/l R45. Some of our experimental results are presented in Fig.6. These data show that the quality of inner capillary surfaces is very important.

The light attenuation length for capillaries of $\emptyset$=20 μm is mainly determined by the bulk transparency of an LS. Obviously, the light attenuation length for $\emptyset$=0.5 mm capillaries filled with 1MN + 3 g/l R45 is about l_{att}=2.87 m and the light attenuation length for ∅=1 mm capillaries filled with 1MN + 3 g/l R45 is l_{att}=3.18 m. Note that the light attenuation length for ∅=20 μm capillaries with mirrors on their far ends is also about l_{att} ≅3.0 m [9].

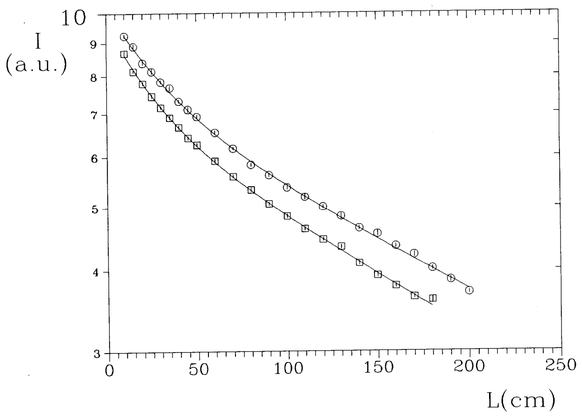

Fig. 5. Influence of R45 dye purity on LSs light attenuation: o – 1MN + 3g/l R45 (high purity), l_{att}=2.87 m and □ - 1MN + 3g/l R45 (low purity), l_{att}=2.33 m.

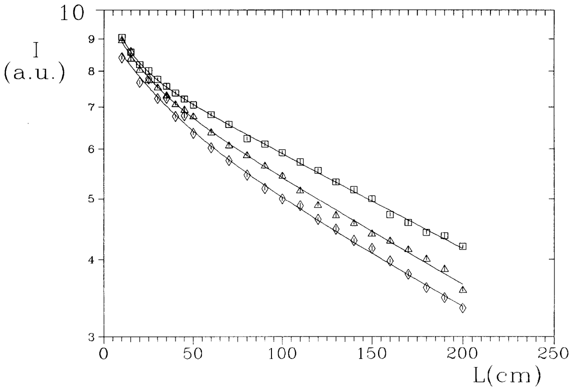

Fig. 6. Influence of inner surface capillaries quality on light attenuation of 1MN + 3g/l R45: □ – capillary C15 (high quality) l_{att}=2.87 m; Δ – capillary C15 (ordinary quality) l_{att}=2.52 m and ◊ – capillary C15 (low quality) l_{att}=2.42 m.

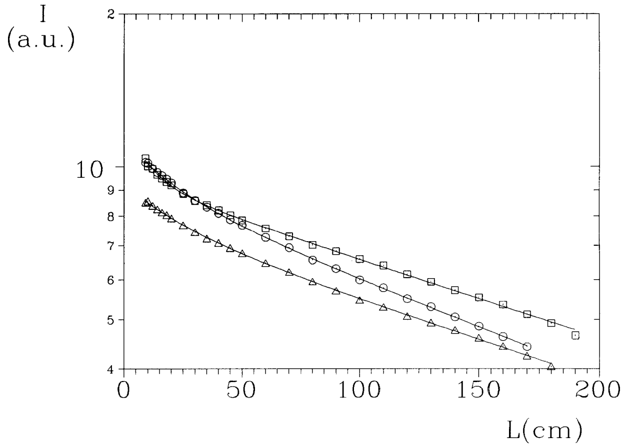

Fig. 7. Influence of 3M-15 dye concentration on light attenuation in LSs based on 1MN: o – 1MN + 6g/l 3M-15 l_{att}=2.29 m; □ – 1MN + 3g/l 3M-15 l_{att}=2.80 m; Δ – 1MN + 1.5g/l 3M-15 l_{att}=2.72 m.

We also investigated the influence of the dye concentration on the light attenuation for capillaries filled with different LSs. Some of our experimental results are presented in Fig.7. Unfortunately, the experimental results presented in Fig.7 were obtained with the use of our ordinary quality capillaries. The experimental results have shown that the chosen concentration of about 3 g/l provides the maximum light output from 2 m capillaries filled with promising LSs.

2.4.2. Comparative study of different LSs

A comparative study of some LSs based on 1MN and IPN is presented in Figs.8-9. As is clear from Figs.8-9, 3M-15 dye provides the best light attenuation lengths l_{att} = 2.85 m and l_{att}=3.19 m for the above solvents (1MN and IPN), respectively. For fiber lengths over 2 m the light output of 1MN + 3g/l 3M-15 is about 13% higher in comparison with 1MN + 3g/l R45. Although for fiber lengths of about 0.1-0.15 m the light output of 1MN + 3g/l R39 is about 23% and 13% higher in comparison with 1MN + 3g/l R45 and 1MN +3g/l 3M-15, respectively. Note that PMP dye has small light attenuation lengths. The light output of IPN + 3g/l 3M-15 from 1.5 m length is about 1.46 times higher than for IPN + 3g/l R45.

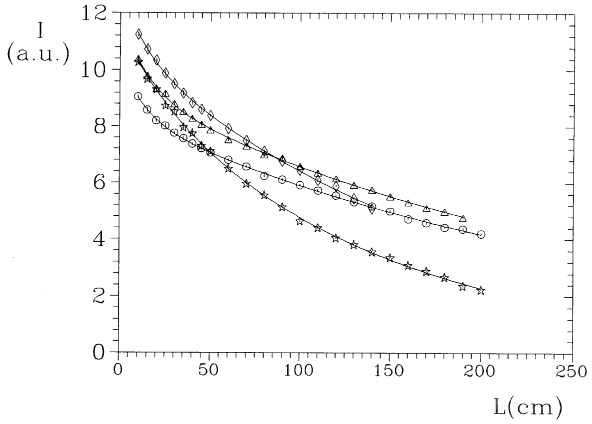

Fig. 8. Light attenuation in 0.5 mm capillaries filled with LSs based on 1MN: Δ – 1MN + 3g/l 3M-15 l_{att}=2.85 m; o – 1MN + 3g/l R45 l_{att}=2.87 m; □ – 1MN + 3g/l R39 l_{att}=1.86 m and ☆ –1MN + 3g/l PMP l_{att}=1.35 m.

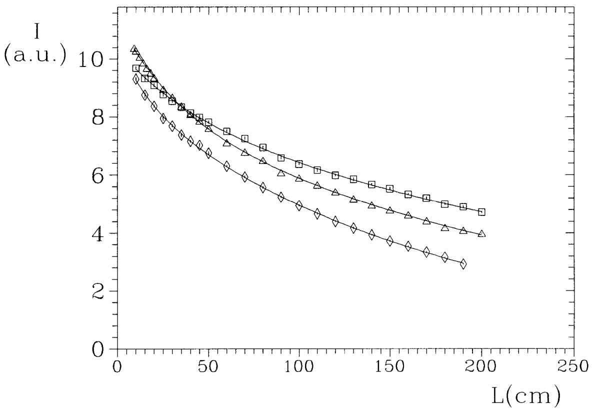

Fig. 9. Light attenuation in 0.5 mm capillaries filled with LSs based on IPN: □ – IPN + 3g/l 3M-15 l_{att}=3.19 m, Δ – IPN + 3g/l R45 l_{att}=2.72 m and ◇ - IPN + 3g/l PMP l_{att}=1.81 m.

A detailed study of light outputs for capillaries filled with our promising LSs based on 1MN and IPN and well known LSs BC-599-13B and BC-599-13G is presented in Fig.10. All these measurements were performed with ∅=0.5 mm quartz capillaries of equal quality. The LS based on BC-599-13G provides the light attenuation length of l_{att}=2.25 m which is lower in comparison with 1MN + 3g/l R45. The light output from 2 m fibers filled with 1MN + 3g/l R45 is about 1.35 time higher in comparison with BC-599-13G and 4.74 times higher than from BC-599-13B.

A comparative study of scintillation properties of liquid-core capillary fibers filled with our promising LSs with some well known plastic scintillating fibers (SCSN-38, λ_{max}=430 nm; Kuraray-3HF, λ_{max}=530 nm) was presented elsewhere [12]. The number of photons N_{ph} versus the length of fibers was measured taking into account the quantum efficiency of the used PM. For equal ∅=0.5 mm capillary fibers filled with 1MN + 3 g/l 3M-15 the light output from 1 m was N_{ph}=30, while for the SCSN-38 fibers was only N_{ph}=9.4 and for the Kuraray-3HF fibers (with double cladding) was N_{ph}=15.6. According to our measurements the light attenuation length for the Kuraray-3HF plastic fibers was about $l_{att} \cong 3.71$ m, while for the liquid-core capillary fibers filled with our best LS – IPN + 3g/l 3M-15 was only l_{att}=3.19 m. Higher values of the light attenuation length for some plastic fibers can not compensate low levels of their light yields in comparison with our best liquid-core capillary fibers. All this only confirms certain advantages of liquid-core capillary fibers.

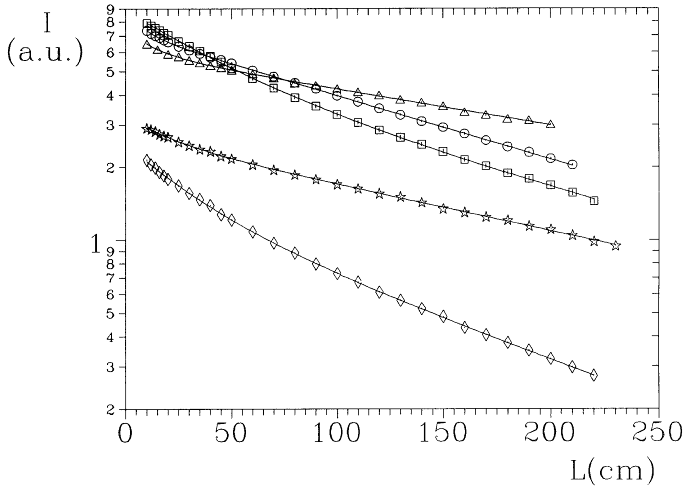

Fig. 10. Light attenuation in 0.5 mm capillaries filled with our new and Bicron LSs: Δ – 1MN + 3g/l R45 l_{att}=2.87 m; □ – 1MN + 3g/l R39 l_{att}=1.44 m; o – 1MN + 3g/l R6 l_{att}=1.63 m, ☆ – BC-599-13G + 3g/l R45 l_{att}=2.25 m and ◊ – BC-599-13B l_{att}=1.29 m.

2.5. Temperature stability of LSs light output

For some applications the temperature stability of LSs light output (in air) is an important factor. We investigated the light output I (in comparison with the standard PS scintillator) of LSs based on 1MN and IPN with our promising dyes versus the temperature (in a region -16^{o}C - +80^{o}C). Fig.11 show some results of this investigation for LSs based on 1MN. It was found that the light output of 1MN + 3g/l R6 and 1MN + 3g/l 3M-15 was practically temperature independent in a region -5 - +20^{o}C. The 1MN+3g/l R6 revealed a highest level of the light output temperature stability of about +0.095%/^{o}C in an interval +20 - +60^{o}C. Similar characteristics we got for LSs based on IPN. Note that the temperature stability of commonly used NE-102a plastic scintillator was about -0.125%/^{o}C in the same temperature interval [16]. The temperature stability of 1MN +3g/l R45 was up to 5.3 times worse in comparison with 1MN+3g/l R6.

2.6. Influence of neutral atmosphere on LSs light output LSs

It is well known that vacuumed LSs have other scintillation properties relative to those in air [17]. We investigated the light output of our LSs in different neutral atmospheres. Some results of this investigation are presented in Fig.12. The initial light output of 1MN + 3g/l R6 in air was taken to be 1. After three hours of evacuation the light output of the LS increased up to a level of 1.27 relative to that in air. Then during two hours we kept the LS in Ar atmosphere (with a technical level of purity) at a pressure of 1.1 atm. Note that at the moment of Ar introduction the light output of the LS slightly dropped to a level of 1.24, but then increased to a level of 1.26. After two hours of the Ar saturation we exposed the LS to the air. As is clear from Fig.12 that the LS light output began to drop to 1.

Practically the similar behavior was observed with the introduction of CO_2 in the vacuumed LS. Note that the introduction of N_2 or Freon–12 (with technical levels of purity) significantly decreased the light output of the vacuumed LS to a level of 1.16.

Vacuumed LSs based on 1MN with our promising dyes like R45, 3M-15 and R39 showed increased levels of the light output of 1.24, 1.24 and 1.32, respectively. Note that vacuumed pure 1MN showed a level of the light output of 2.0 relative to that in air. It is evident that the above promising dyes are not optimal for LSs in neutral atmospheres.

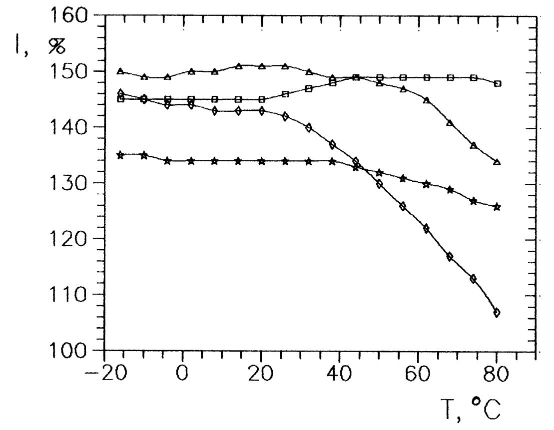

Fig. 11. Light output of some LSs based on 1MN versus temperature: □ – 1MN + 3g/l R6; ◊ – 1MN + 3g/l R45, Δ –1MN + 3g/l R39 and ☆ – 1MN + 3g/l 3M-15.

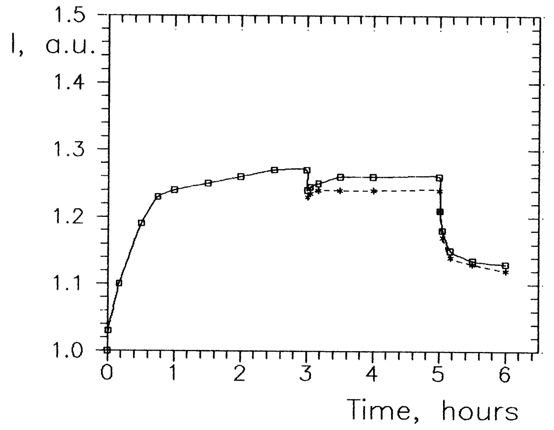

Fig. 12. Light output of 1MN + 3g/l R6 in some neutral atmospheres. Solid line - for Ar, dashed line - for CO_2.

Conclusion

A study on optical and luminescent characteristics of some LSs has been performed. The investigation results of about 60 new scintillating dyes and 8 solvents are being presented. LSs based on 1-methylnaphthalene and a new solvent IPN containing R6, R45, R39 and 3M-15 dyes have shown the scintillation efficiency up to 34-52% higher in comparison with the standard PS scintillator. Dyes concentration of about 3g/l is optimal versus the light yield, light attenuation length and light emission locality. Our promising LSs revealed relatively short main decay time constants of about 6.2-7.6 ns and in this case their light pulses durations are comparative with commonly used green plastic scintillators.

The importance of high quality of purification of solvents and dyes, high optical quality of the inner surfaces of capillaries and a special procedure of capillary treatment for high values of the light attenuation length (≥ 3 m) has been ascertained. Liquid-core capillary fibers filled with 1MN + 3 g/l R45 provide 1.35 times higher light output at a distance of about 1 m than that of fibers filled with BC-599-13G. Capillaries filled with 1MN + 3 g/l 3M-15 at a distance of about 2 m provide 1.9 times higher light output than that of Kuraray-3HF (with double cladding) plastic scintillating fibers.

The temperature stability of 1MN+3g/l R6 liquid scintillator is about 0.095%/^{o}C in an interval +20 – +60^{o}C. Some vacuumed liquid scintillators based on 1-methylnaphthalene have enhanced levels of the scintillation efficiency up to 24-32% relative to those in air.

Large attenuation lengths, high light output, excellent radiation resistance [10] show that new LSs and capillary systems filled with LSs are very promising for tracking detectors and calorimetry application.

Acknowledgements

The authors express their gratitude to A.I.Peresypkin for his help in measurements and V.A.Kozlov for providing them with tetraphenyl lead.

References

[1] Golovkin S.V. et al.//Nucl. Instr. and Meth. A305 (1991) 385.

[2] Denisov A.G. et al. //Nucl. Instr. and Meth. A310 (1991) 479.

[3] Bähr J. al.//Nucl. Instr. and Meth. A306 (1991) 169.

[4] Adinolfi M. al.//Nucl. Instr. and Meth. A311 (1992) 91.

[5] Adinolfi M. al.//Nucl. Instr. and Meth. A315 (1992) 177.

[6] Bozhko N.I. et al.//Nucl. Instr. and Meth. A317 (1992) 97.

[7] Cianfarani C. et al.//Nucl. Instr. and Meth. A339 (1994) 449.

[8] Cardini A. et al.//Nucl. Instr. and Meth. A346 (1994) 163.

[9] Buontempo S. et al.//Nucl. Instr. and Meth. A360 (1995) 7.

[10] Golovkin S.V. et al.//Nucl. Instr. and Meth. A362 (1995) 283.

[11] Annis P. et al. "Experimental reasults from large volume active target made of glass capillaries and liquid scintillator". Contribution to 95 Wire Chambers Conference: Recent Trends and Alternative Techniques, Vienna, Austria, February 13-17, 1995 (to be published in the Proc. of the Conference).

[12] Cardini A. et al.//Nucl. Instr. and Meth. A361 (1995) 129.

[13] Lewis O. et al.//Rev. Sci. Instr. 44 (1973) 107.

[14] Birks J.B.. – In "The theory and Practice of Scintillation Counting" Pergamon publ., New York, 1964.

[15] Angelini C. et al. Preprint CERN-EP/89-120, Geneva 1989.

[16] Nuclear Enterprises (G.B.) LTD Catalogue 1967, p.5.

[17] M.N.Medvedev in Proc. of VI All Union Conference on synthesize, production and application of scintillators, 26-28 May 1971 Khar'kov. Ed. Yu.A. Tsyrlin, Cheboksary publ., 1972, p.269 (in Russian).

Received February 22, 1996

Appendix

List of investigated solvents, luminophores and dopants

1MN – 1-methylnaphthalene
IPN – new solvent
1PN – 1-phenylnaphthalene
IBP – 1-isopropylbiphenyl
1CLN – 1-clornaphthalene
1MON – 1-methoxynaphthalene
DIPN – 1,4-diisopropylnaphthalene
HnTP – hydrogenated-n-terphenyl
TPT – tetraphenyl tin
TPL – tetraphenyl lead
DBNB – 1,2-dibrome-4-nitrobenzole, n_{core}=1.984
N – naphthalene
pTP – paraterphenyl, λ_{abs}=275 nm, λ_{em}=340 nm
POPOP – 1,4-bis-(2-(5-phenyloxazolyl))-benzene, λ_{abs}=365 nm, λ_{em}=420 nm
oPOPOP – 1,2-bis-(2-(5-phenyloxazolyl))-benzene, λ_{abs}=310-330 nm, λ_{em}=420 nm
DMPOPOP – 1,4-di-2-(4-methyl-(5-phenyloxazolyl))-benzene, λ_{abs}=370 nm, λ_{em}=430 nm
vPOPOP – vinylPOPOP, $\lambda_{em} \cong$420 nm
BDPAD – 2-biphenyl-5-(4'-diethylaminophenyl)-1,3,4-oxadiazole, λ_{em}=500 nm
BDPD – oxadiazole derivative, $\lambda_{em} \cong$500 nm
PMP – 1-phenyl-3-mezityl-2-pyrazoline, λ_{em}=420 nm
bis-DAPD – 2,5-bis-(4-dimethylaminophenyl)-1,3,4-oxadiazole, λ_{em}=400 nm
SFPDMAPO – (4-sulfofluoridophenyl)-5-(4"-dimethylaminophenyl) -1,3,4- oxazole, λ_{em}=513 nm
BPEA – 9,10-bis-(phenylethyl)-anthracene, λ_{abs}=470 nm, λ_{em}=505 nm
CLBPEA – 2-clor-9,10-bis-(phenylethyl)-anthracene, λ_{abs}=480 m, λ_{em}=525 nm

DMBPEA – 1,4-dimeth4yl-9,10-bis-(phenylethyl)-anthracene, λ_{em}=540 nm
K-7 – 7-diethylamino-3-(methylbenzimidazolyl-2’)-coumarin, λ_{em}=510 nm
K-30 – 7-diethylamino-3-(3’-methylbenzimidazolyl-2’)-coumarin, λ_{em}=480 nm
DSP – 1,5-diphenyl-3-styryl-2-pyrazoline, λ_{em}=460 nm
DPA – diphenylanthracene, λ_{em}=420 nm
X25 – 4-morpholinyl-naphthalic anhydride, λ_{abs}=400 nm, λ_{em}=480 nm
X26 – naphthalimide derivative, $\lambda_{em} \cong$490 nm
X27 – naphthalimide derivative, $\lambda_{em} \cong$490 nm
X31 – 4-morpholinyl-N-phenylnaphthalimide, λ_{abs}=390 nm, λ_{em}=490 nm
X42 – naphthalimide derivative, $\lambda_{em} \cong$490 nm
X43 – naphthalimide derivative, $\lambda_{em} \cong$490 nm
X44 – naphthalimide derivative, $\lambda_{em} \cong$490 nm
R2 – pyrazoline derivative, λ_{em} = 480 nm
R6 – pyrazoline derivative, λ_{em} = 485 nm
R39 – pyrazoline derivative, λ_{em}=495 nm
R40 – 2-(4’,8’-dimethoxinaphthyl)-6-diethylamino-benzoxazole, λ_{em}=495 nm
R45 – pyrazoline derivative, λ_{abs}=390 nm, λ_{em} = 500 nm
R49 – (1-cyan-2,4-diphenylpyrido-1,2 [a])-benzimidazole, λ_{abs}=400 nm, λ_{em}=530 nm
R63 – 1-(2’-methoxyphenyl)-3-(4”-bromophenyl)-5-phenyl- pyrazoline, λ_{abs}=390 nm, λ_{em}=510 nm
R6-J – 1-(2’-methoxyphenyl)-3-(4”-iodophenyl)-5-phenyl- pyrazoline, λ_{abs}=390 nm, λ_{em}=490 nm
R-911 – benzoxazole derivative, λ_{abs}=380 nm, λ_{em}=490 nm
R-912 – (2’-phenyl-4’-anthracyl-benz)-1,2-benzimidazole, λ_{em}=480 nm
R-913 – benzoxazole derivative, λ_{em}=500 nm
R-914 – 2-anthracyl-7-diethylamino-benzoxazole, λ_{em}=570 nm
PPPyr – pyrazoline derivative, $\lambda_{em} \cong$500 nm
BPPyr – 1,3-biphenyl-2-pyrazoline, λ_{abs}=364 nm, λ_{em}=450 nm
TPB – 1,1’,4,4’-tetraphenylbutadiene, λ_{abs}=340 nm, λ_{em}=435 nm
L7 – 4-methoxyphenyl-2-(3,4-dihydro-2-quinolene-3) oxazole, $\lambda_{em} \cong$500 nm
L8 – α-(anthryl-9)-4-(5-phenyloxadiazolyl-2)-styrene, $\lambda_{em} \cong$500 nm
L9 – α-(anthryl-9)-4-(5-biphenyloxadiazolyl-2)-styrene, $\lambda_{em} \cong$500 nm
L10 – 9,10-di (methylaniline) anthracene, λ_{em}=530 nm
L11 – 4-methoxyphenyl-2 (hexahydrochroman-3-yl-2-on)-oxadiazole, $\lambda_{em} \cong$430 nm
L13 – α-(4-methoxyphenyloxazolyl-2)-4 (-4-phenyloxazolyl-2) styrene, $\lambda_{em} \cong$500 nm
L15 – naphthoylenebenzimidazole, λ_{em}=450 nm
K-27 – benzoxanthene derivative, λ_{em}=500 nm
P-26 – thioxanthene derivative, λ_{em}=530 nm
3HF – 3-hydroxiflavone, λ_{em}=530 nm
OPBPP – 3-[(2’-oxaphenanthrenyl)-benzimidazolyl-5’]-5-phenyl-2-pyrazoline, λ_{em}=480 nm

OPBD – (2'-oxaphenanthrenyl)-benzimidazole, λ_{em}=490 nm
3M-15 – pyrazoline derivative, λ_{abs}=360 nm, λ_{em}=490 nm
OP-45 – pyrazoline derivative, $\lambda_{em} \cong$500 nm
N/116 – 2-(biphenyl)-5-(oxaphenyl-2)-thiazole, λ_{em}=500 nm
N/118 – 2-(oxaphenyl-2)-quinolinyloxazole, $\lambda_{em} \cong$500 nm
N/119 – 2,5-bis-(5'-phenyloxazolyl)-phenol, $\lambda_{em} \cong$500 nm
N/120 – 2-(4'-diethylaminophenyl)-N'-methyl-2- oxaquinolinyloxazole, $\lambda_{em} \cong$500 nm
N/266 – 2-(4'-sulfofluoridomethylphenyl)-5-(4"- dimethylaminophenyl)-1,3,4-oxadiazole, λ_{em}=440 nm.

В.Г.Васильченко и др.
Новые жидкие сцинтилляторы для детекторов частиц на основе капиллярных волокон.

Оригинал-макет подготовлен с помощью системы LaTeX.
Редактор Е.Н.Горина. Технический редактор Н.В.Орлова.

Подписано к печати 23.02.96. Формат 60 × 84/8. Офсетная печать.
Печ.л. 2.12. Уч.-изд.л. 1.63. Тираж 250. Заказ 676. Индекс 3649.
ЛР №020498 17.04.97.

ГНЦ РФ Институт физики высоких энергий
142284, Протвино Московской обл.

Индекс 3649

ПРЕПРИНТ 96-13, ИФВЭ, 1996
